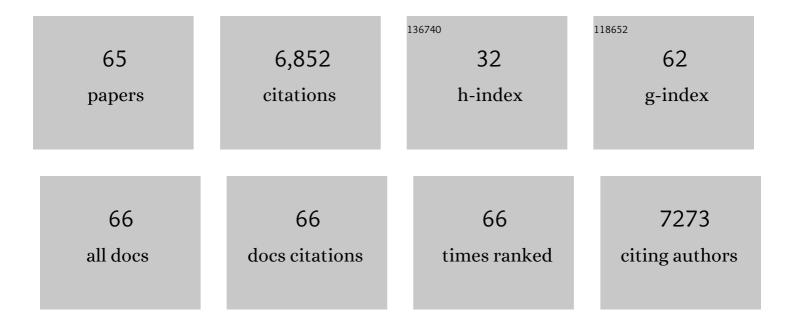
## Andrea Zitolo

List of Publications by Year in descending order

Source: https://exaly.com/author-pdf/3442882/publications.pdf Version: 2024-02-01



#	Article	IF	CITATIONS
1	Identification of catalytic sites for oxygen reduction in iron- and nitrogen-doped grapheneÂmaterials. Nature Materials, 2015, 14, 937-942.	13.3	1,714
2	Activity–Selectivity Trends in the Electrochemical Production of Hydrogen Peroxide over Single-Site Metal–Nitrogen–Carbon Catalysts. Journal of the American Chemical Society, 2019, 141, 12372-12381.	6.6	493
3	Identification of catalytic sites in cobalt-nitrogen-carbon materials for the oxygen reduction reaction. Nature Communications, 2017, 8, 957.	5.8	443
4	Electroreduction of CO <sub>2</sub> on Singleâ€Site Copperâ€Nitrogenâ€Doped Carbon Material: Selective Formation of Ethanol and Reversible Restructuration of the Metal Sites. Angewandte Chemie - International Edition, 2019, 58, 15098-15103.	7.2	369
5	Identification of durable and non-durable FeNx sites in Fe–N–C materials for proton exchange membrane fuel cells. Nature Catalysis, 2021, 4, 10-19.	16.1	368
6	Electrochemical Reduction of CO <sub>2</sub> Catalyzed by Fe-N-C Materials: A Structure–Selectivity Study. ACS Catalysis, 2017, 7, 1520-1525.	5.5	363
7	P-block single-metal-site tin/nitrogen-doped carbon fuel cell cathode catalyst for oxygen reduction reaction. Nature Materials, 2020, 19, 1215-1223.	13.3	278
8	High loading of single atomic iron sites in Fe–NC oxygen reduction catalysts for proton exchange membrane fuel cells. Nature Catalysis, 2022, 5, 311-323.	16.1	248
9	Revised Ionic Radii of Lanthanoid(III) Ions in Aqueous Solution. Inorganic Chemistry, 2011, 50, 4572-4579.	1.9	212
10	Evolution Pathway from Iron Compounds to Fe <sub>1</sub> (II)–N <sub>4</sub> Sites through Gas-Phase Iron during Pyrolysis. Journal of the American Chemical Society, 2020, 142, 1417-1423.	6.6	185
11	Degradation by Hydrogen Peroxide of Metal-Nitrogen-Carbon Catalysts for Oxygen Reduction. Journal of the Electrochemical Society, 2015, 162, H403-H414.	1.3	161
12	On the Influence of Oxygen on the Degradation of Feâ€N  Catalysts. Angewandte Chemie - International Edition, 2020, 59, 3235-3243.	7.2	160
13	Volcano Trend in Electrocatalytic CO <sub>2</sub> Reduction Activity over Atomically Dispersed Metal Sites on Nitrogen-Doped Carbon. ACS Catalysis, 2019, 9, 10426-10439.	5.5	142
14	On the Influence of Oxygen on the Degradation of Feâ€N  Catalysts. Angewandte Chemie, 2020, 132, 3261-3269.	1.6	133
15	Physical and Chemical Considerations for Improving Catalytic Activity and Stability of Non-Precious-Metal Oxygen Reduction Reaction Catalysts. ACS Catalysis, 2018, 8, 11264-11276.	5.5	101
16	Analysis of the Detailed Configuration of Hydrated Lanthanoid(III) Ions in Aqueous Solution and Crystalline Salts by Using K―and L <sub>3</sub> â€Edge XANES Spectroscopy. Chemistry - A European Journal, 2010, 16, 684-692.	1.7	73
17	Effect of Pyrolysis Atmosphere and Electrolyte pH on the Oxygen Reduction Activity, Stability and Spectroscopic Signature of FeN <sub>x</sub> Moieties in Fe-N-C Catalysts. Journal of the Electrochemical Society, 2019, 166, F3311-F3320.	1.3	70
18	Carbonâ€Nanotubeâ€Supported Copper Polyphthalocyanine for Efficient and Selective Electrocatalytic CO <sub>2</sub> Reduction to CO. ChemSusChem, 2020, 13, 173-179.	3.6	60

ANDREA ZITOLO

#	Article	IF	CITATIONS
19	Cuprizone neurotoxicity, copper deficiency and neurodegeneration. NeuroToxicology, 2010, 31, 509-517.	1.4	59
20	Oxygen reduction reaction mechanism and kinetics on M-NxCy and M@N-C active sites present in model M-N-C catalysts under alkaline and acidic conditions. Journal of Solid State Electrochemistry, 2021, 25, 45-56.	1.2	59
21	Oxygen Reduction Reaction in Alkaline Media Causes Iron Leaching from Fe–N–C Electrocatalysts. Journal of the American Chemical Society, 2022, 144, 9753-9763.	6.6	59
22	The origin of the high electrochemical activity of pseudo-amorphous iridium oxides. Nature Communications, 2021, 12, 3935.	5.8	56
23	Using a Combined Theoretical and Experimental Approach to Understand the Structure and Dynamics of Imidazolium-Based Ionic Liquids/Water Mixtures. 1. MD Simulations. Journal of Physical Chemistry B, 2013, 117, 12505-12515.	1.2	53
24	Structural Investigation of Lanthanoid Coordination: a Combined XANES and Molecular Dynamics Study. Inorganic Chemistry, 2009, 48, 10239-10248.	1.9	51
25	Using a Combined Theoretical and Experimental Approach to Understand the Structure and Dynamics of Imidazolium-Based Ionic Liquids/Water Mixtures. 2. EXAFS Spectroscopy. Journal of Physical Chemistry B, 2013, 117, 12516-12524.	1.2	50
26	Non-precious metal cathodes for anion exchange membrane fuel cells from ball-milled iron and nitrogen doped carbide-derived carbons. Renewable Energy, 2021, 167, 800-810.	4.3	50
27	Electroreduction of CO <sub>2</sub> on Singleâ€Site Copperâ€Nitrogenâ€Doped Carbon Material: Selective Formation of Ethanol and Reversible Restructuration of the Metal Sites. Angewandte Chemie, 2019, 131, 15242-15247.	1.6	43
28	Hydration Properties of the Zn <sup>2+</sup> Ion in Water at High Pressure. Inorganic Chemistry, 2013, 52, 1141-1150.	1.9	41
29	Designing the 3D Architecture of PGM-Free Cathodes for H <sub>2</sub> /Air Proton Exchange Membrane Fuel Cells. ACS Applied Energy Materials, 2019, 2, 7211-7222.	2.5	41
30	Influence of the Second Coordination Shell on the XANES Spectra of the Zn <sup>2+</sup> Ion in Water and Methanol. ChemPlusChem, 2012, 77, 234-239.	1.3	40
31	Synergy between molybdenum nitride and gold leading to platinum-like activity for hydrogen evolution. Physical Chemistry Chemical Physics, 2015, 17, 4047-4053.	1.3	38
32	Metal Oxide Clusters on Nitrogen-Doped Carbon are Highly Selective for CO <sub>2</sub> Electroreduction to CO. ACS Catalysis, 2021, 11, 10028-10042.	5.5	37
33	Potentialâ€Induced Spin Changes in Fe/N/C Electrocatalysts Assessed by In Situ Xâ€ray Emission Spectroscopy. Angewandte Chemie - International Edition, 2021, 60, 11707-11712.	7.2	36
34	Effect of the Zn <sup>2+</sup> and Hg <sup>2+</sup> lons on the Structure of Liquid Water. Journal of Physical Chemistry A, 2011, 115, 4798-4803.	1.1	34
35	Stable Cr-MFI Catalysts for the Nonoxidative Dehydrogenation of Ethane: Catalytic Performance and Nature of the Active Sites. ACS Catalysis, 2021, 11, 3988-3995.	5.5	34
36	Structural characterization of zinc(II) chloride in aqueous solution and in the protic ionic liquid ethyl ammonium nitrate by x-ray absorption spectroscopy. Journal of Chemical Physics, 2011, 135, 154509.	1.2	33

ANDREA ZITOLO

#	Article	IF	CITATIONS
37	Stabilization of Iron-Based Fuel Cell Catalysts by Non-Catalytic Platinum. Journal of the Electrochemical Society, 2018, 165, F1084-F1091.	1.3	33
38	Timeâ€Resolved Potentialâ€Induced Changes in Fe/N/Câ€Catalysts Studied by In Situ Modulation Excitation Xâ€Ray Absorption Spectroscopy. Advanced Energy Materials, 2022, 12, .	10.2	33
39	Effects of the Pathological Q212P Mutation on Human Prion Protein Non-Octarepeat Copper-Binding Site. Biochemistry, 2012, 51, 6068-6079.	1.2	32
40	X-Ray absorption spectroscopy investigation of 1-alkyl-3-methylimidazolium bromide salts. Journal of Chemical Physics, 2011, 135, 074505.	1.2	31
41	Au and Pt Remain Unoxidized on a CeO <sub>2</sub> -Based Catalyst during the Water–Gas Shift Reaction. Journal of the American Chemical Society, 2022, 144, 446-453.	6.6	31
42	Design of polygalacturonate hydrogels using iron(II) as cross-linkers: A promising route to protect bioavailable iron against oxidation. Carbohydrate Polymers, 2018, 188, 276-283.	5.1	27
43	Enhancing the electrocatalytic activity of Fe phthalocyanines for the oxygen reduction reaction by the presence of axial ligands: Pyridine-functionalized single-walled carbon nanotubes. Electrochimica Acta, 2021, 398, 139263.	2.6	27
44	Tuning the Structure of Galacturonate Hydrogels: External Gelation by Ca, Zn, or Fe Cationic Cross-Linkers. Biomacromolecules, 2019, 20, 2864-2872.	2.6	25
45	X-ray Absorption Study of the Solvation Structure of Cu <sup>2+</sup> in Methanol and Dimethyl Sulfoxide. Inorganic Chemistry, 2012, 51, 8827-8833.	1.9	23
46	Water-Mediated ElectroHydrogenation of CO <sub>2</sub> at Near-Equilibrium Potential by Carbon Nanotubes/Cerium Dioxide Nanohybrids. ACS Applied Energy Materials, 2020, 3, 8509-8518.	2.5	23
47	The Challenge of Achieving a High Density of Fe-Based Active Sites in a Highly Graphitic Carbon Matrix. Catalysts, 2019, 9, 144.	1.6	22
48	Understanding how single-atom site density drives the performance and durability of PGM-free Fe–N–C cathodes in anion exchange membrane fuel cells. Materials Today Advances, 2021, 12, 100179.	2.5	18
49	In Situ Observation of the Formation and Structure of Hydrogen-Evolving Amorphous Cobalt Electrocatalysts. ACS Energy Letters, 2017, 2, 2545-2551.	8.8	17
50	K-edge XANES investigation of octakis(DMSO)lanthanoid(iii) complexes in DMSO solution and solid iodides. Physical Chemistry Chemical Physics, 2013, 15, 8684.	1.3	15
51	Evidence for an egg-box-like structure in iron( <scp>ii</scp> )–polygalacturonate hydrogels: a combined EXAFS and molecular dynamics simulation study. Physical Chemistry Chemical Physics, 2020, 22, 2963-2977.	1.3	14
52	Aerosol synthesis of thermally stable porous noble metals and alloys by using bi-functional templates. Materials Horizons, 2020, 7, 541-550.	6.4	13
53	On the possibility of using XANES to investigate bromide-based ionic liquids. Chemical Physics Letters, 2014, 591, 32-36.	1.2	12
54	X-ray absorption spectroscopy study of the solvation structure of zinc(II) in dimethyl sulfoxide solution. Chemical Physics Letters, 2010, 499, 113-116.	1.2	10

ANDREA ZITOLO

#	Article	IF	CITATIONS
55	Changes in structure and conduction type upon addition of Ir to ZnO thin films. Thin Solid Films, 2017, 636, 694-701.	0.8	10
56	Ion hydration in high-density water. Journal of Physics: Conference Series, 2009, 190, 012057.	0.3	9
57	Self-Assembly of the Nonplanar Fe(III) Phthalocyanine Small-Molecule: Unraveling the Impact on the Magnetic Properties of Organic Nanowires. Chemistry of Materials, 2018, 30, 879-887.	3.2	9
58	Measurement of x-ray multielectron photoexcitations at the <mml:math xmlns:mml="http://www.w3.org/1998/Math/MathML" display="inline"&gt;<mml:mrow><mml:msup><mml:mtext>I</mml:mtext><mml:mo>â^`</mml:mo></mml:msup><n Physical Review B, 2008, 78, .</n </mml:mrow></mml:math 	ıml:mtext	>â <sup>&amp;</sup> ‰
59	Revisiting the Sodiation Mechanism of TiO2 via Operando X-ray Absorption Spectroscopy. Applied Sciences (Switzerland), 2020, 10, 5547.	1.3	7
60	The local atomic structure and thermoelectric properties of Ir-doped ZnO: hybrid DFT calculations and XAS experiments. Journal of Materials Chemistry C, 2021, 9, 4948-4960.	2.7	7
61	Potentialâ€Induced Spin Changes in Fe/N/C Electrocatalysts Assessed by In Situ Xâ€ray Emission Spectroscopy. Angewandte Chemie, 2021, 133, 11813-11818.	1.6	5
62	Fe-heme structure in Cu,Zn superoxide dismutase from Haemophilus ducreyi by X-ray Absorption Spectroscopy. Archives of Biochemistry and Biophysics, 2010, 498, 43-49.	1.4	3
63	Short range order of As40-xCuxTe60 glasses. Journal of Non-Crystalline Solids, 2018, 481, 202-207.	1.5	1
64	Structural Characterization of Ionic Liquids by X-Ray Absorption Spectroscopy. Soft and Biological Matter, 2014, , 149-172.	0.3	0
65	Pure silica-supported transition metal catalysts for the non-oxidative dehydrogenation of ethane: confinement effects on the stability. Journal of Materials Chemistry A, 0, , .	5.2	0